

# Isothermal Crystallization Kinetics of Polypropylene by Differential Scanning Calorimetry. I. Experimental Conditions

Fernando Hernández-Sánchez,<sup>1</sup> Luis F. del Castillo,<sup>2</sup> Ricardo Vera-Graziano<sup>2</sup>

<sup>1</sup>Centro de Investigación Científica de Yucatán, A. P. 87, Cordemex, Mérida, Yucatán, Mexico

<sup>2</sup>Instituto de Investigaciones en Materiales, UNAM, A. P.70-360, Coyoacán 04510, D.F. Mexico

Received 9 June 2003; accepted 14 August 2003

**ABSTRACT:** Reliable isothermal crystallization kinetic studies can be achieved by differential scanning calorimetric techniques only under restricted conditions. In the case of isotactic polypropylene, our results indicate that those conditions are met in the range of 3°C below the isothermal crystallization temperature  $T_c$ . Experimentally, it is only in this range when the complete crystallization peak can be registered by the DSC and depicted in a thermogram. Just around this temperature interval, the Avrami exponent  $n$

= 3 for bulk crystallization, whereas for any other test the isothermal temperature  $T_{it}$ , nonisothermal conditions prevail and the Avrami exponent deviates from the expected value. © 2004 Wiley Periodicals, Inc. *J Appl Polym Sci* 92: 970–978, 2004

**Key words:** crystallization; kinetics (polym.); isothermal crystallization; differential scanning calorimetry (DSC); Avrami parameters

## INTRODUCTION

The kinetics of polymer crystallization is closely related to microstructure and thermal history.<sup>1</sup> Kinetic crystallization experiments under isothermal regime involve the consideration of inherent characteristics, such as the differences in the heat capacities ( $\Delta C_p$ ) and in heat diffusion rates ( $\Delta\kappa$ ) of the polymer and the oven or thermal chamber of the equipment. To work under true isothermal conditions also involves careful analysis on the experimental procedure, the degree of temperature control, and the determination of the test temperature at which the isothermal experiment will be conducted, designated here as the test isothermal temperature ( $T_{it}$ ).

The usual procedure for an isothermal experiment requires first melting the material well above its crystallization temperature to ensure a homogeneous liquid state in the sample. In the case of polymers this condition is obtained above the liquid–liquid transition ( $ll$ -transition).<sup>2</sup> After stabilization above the  $ll$ -transition, the temperature is reduced at the highest cooling rate to the test isothermal temperature  $T_{it}$ . This temperature should be constant during the preset crystallization process. It is usually assumed that the DSC apparatus meet the described conditions. How-

ever, several factors should be considered previously to obtain reliable data.

Apparently, a differential scanning calorimeter (DSC), with minimum thermal inertia (a small DSC oven), meets the required conditions to study polymer crystallization kinetics. The DSC techniques also assume that the small size of the sample minimizes the time to equalize the temperature of the sample with that of the DSC oven. However, the differences in heat capacities ( $\Delta C_p$ ) and in heat diffusion rates ( $\Delta\kappa$ ) of the polymer and the DSC oven cause the DSC oven to reach the test temperature before the sample. This kinetic effect should be considered when isothermal crystallization studies are made by DSC.

The aim of this study was to analyze the effects of inherent and experimental conditions to determine limits for studying the kinetics crystallization on polymers under isothermal conditions, by DSC techniques. We report here such conditions for isotactic polypropylene (*iPP*).

The development of crystallinity is associated with the exothermic peak obtained in DSC measurements. This peak is integrated to calculate the degree of crystallinity assuming proportionality between the rate of crystallization and the heat flow.<sup>3</sup> The mass fraction of crystallinity  $X$ , as a function of time, is described by the Avrami equation and can be used to study the isothermal crystallization kinetics on polymers:

$$\log[-\ln(1 - X)] = \log K + n \log(t) \quad (1)$$

where  $n$  is the Avrami exponent,  $K$  is the kinetic constant, and  $t$  is the crystallization time. The param-

Correspondence to: R. Vera-Graziano.

Contract grant sponsor: DGAPA-UNAM; contract grant number: IN107502.

TABLE I  
Molecular Weights of Polypropylene Standards

PP	$M_w$ (g mol <sup>-1</sup> g <sup>-1</sup> )	$M_n$ (g mol <sup>-1</sup> g <sup>-1</sup> )	PD
1	50,400	26,600	1.9
2	151,900	38,400	4.0
3	348,300	32,500	10.7

eters  $K$  and  $n$  depend on the polymer structure and the type of spatial crystallization dimensions, respectively, and can be used to interpret qualitatively the nucleation mechanism, effect of morphology, and the overall crystallization rate of the material.

Bulk crystallization of pure polymers is tridirectional and consequently the theoretical value of the Avrami exponent  $n$  should be 3. However, reported values of  $n$  range above and below 3.<sup>4-6</sup> These variations can be attributed to several causes, mainly deviations from the isothermal conditions, as discussed below.

## EXPERIMENTAL

### Materials

The *i*PP samples were standards from American Polymer Standards Co. (Mentor, OH). The molecular weights and polydispersities of the samples are shown in the Table I.

Chemical structure and tacticity of the *i*PP samples were determined by NMR and WAXD (discussed below). Solid-state <sup>13</sup>C CP/MAS (cross polarization and magic-angle spinning) NMR spectra were acquired on a Bruker Avance 400 spectrometer (Billerica, MA), operating at 100 MHz. The MAS rate for the 4-mm rotor was 5 kHz to eliminate spinning side bands, and with TMS as an external reference. The WAXD spectra were recorded on a Bruker axs, Model D8, Advance (Madison, WI), operating with Cu-K<sub>α</sub> radiation at a scan speed of 1° 2θ/min.

### Sample preparation

In a DSC aluminum pan (Perkin Elmer Cetus Instruments, Norwalk, CT) the sample, about 3 mg, was heated to 200°C to mold-in the polymer to ensure full contact with the inner surface of pan. The pan was then sealed and cooled.

### DSC isothermal kinetic experiment

The experiments were conducted using a Perkin-Elmer DSC-7, with a computerized data-acquisition system. The DSC was set to run the experiments under the following conditions. The sample, under nitrogen atmosphere, was heated to 250°C. After 10 min at this

temperature the system was cooled at a rate of 450°C/min to the selected test isothermal temperature  $T_{it}$ . This temperature was kept constant and the heat flow was monitored as a function of time.

## RESULTS AND DISCUSSION

### Effect of test isothermal temperature

We first studied the effect of the test isothermal temperature  $T_{it}$  on crystallization kinetics. The heat flow versus time isotherms at four  $T_{it}$  are shown in Figure 1(A) to (D) for the *i*PP sample of MW 151,900. Each plot shows the crystallization peak and the inset, the complete thermogram. The vertical dashed lines show the oven-stabilization time, indicating the time needed for stabilization of the DSC oven after the  $T_{it}$  is reached.

As may be observed in Figure 1, both the height of the crystallization peaks and the DSC oven-stabilization time decrease as the  $T_{it}$  increases, and, as expected, the time for complete crystallization increases with  $T_{it}$ . For example, at 100°C [Fig. 1(A)], the crystallization peak increased to 14.63 W/g and the crystallization time is 40 s, whereas at 129°C [Fig. 1(D)], these values are 0.082 W/g and 785 s, respectively. Furthermore, the area under the peak decreases as the  $T_{it}$  increases in this range of temperatures.

To evaluate properly the Avrami parameters it is necessary to register the complete crystallization peak. According to Figure 1, this condition is fulfilled only at 129°C [Fig. 1(D)]. At lower  $T_{it}$  [Fig. 1(A)-(C)], the initial part of the crystallization peak is not observed because polymer crystallization started before the DSC oven was stabilized. In these cases, an extrapolation to the initial part of the peak was necessary to estimate the Avrami parameters.

In contrast, at a  $T_{it}$  of 130°C the crystallization peak looks different, as shown for two *i*PP samples of different MW [Fig. 2(A): 151,900 and (B): 50,400]. For both samples the initial part and the maximum of the crystallization peak are clearly observed, although the end of the crystallization peaks do not fall to zero heat flow; the curves rise again after passing the maximum, possibly because of polymer melting and recrystallization. Therefore, the DSC in only a very short range can register true isothermal crystallization conditions. The limits of this range may be affected by the molecular weight as depicted in Figure 2(B) for the *i*PP of MW 50,400, although molecular weight effects are discussed in the following section.

The minimum temperature at which the crystallization peak is completely registered is designated here as the DSC isothermal crystallization temperature— $T_c^*$ . For the sample of MW 151,900 the  $T_c^*$  can be taken as 129°C.

Figure 3(A) shows the Avrami plots obtained at different  $T_{it}$ . The mass fractions of crystallinity [ $X$  in

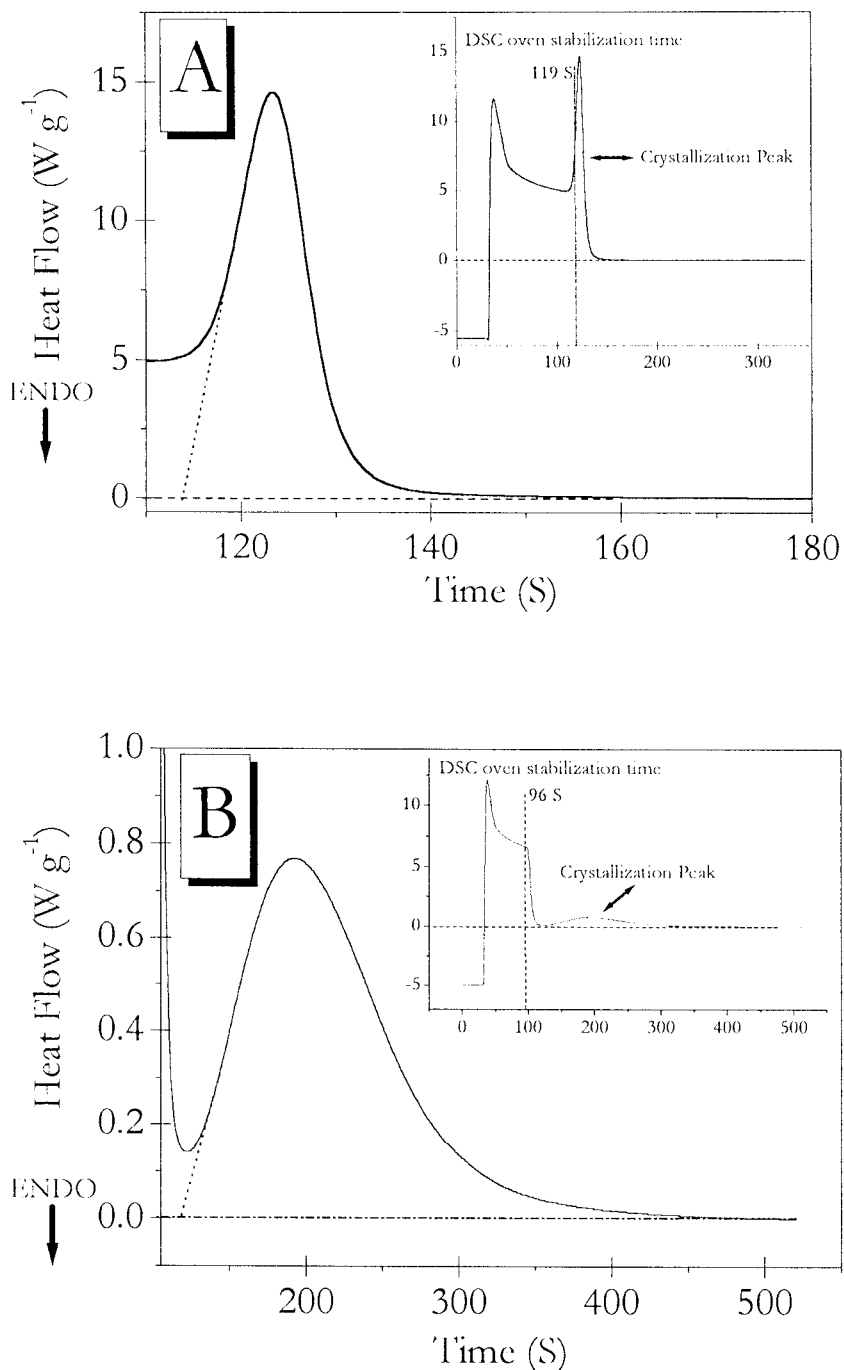


**Figure 1** Thermograms of the crystallization of *i*PP of MW 151,900, at four  $T_{it}$ : (A) 100°C, (B) 120°C, (C) 126°C, (D) 129°C. The main plots correspond to the crystallization peak and the inset to the original thermogram.

eq. (1)] were calculated considering the area below the curve at a given time divided by the total area under the peak. The Avrami parameters  $n$  and  $K$  were calculated in linear intervals [Fig. 3(B)]. The time interval involved in each straight line coincides with the time interval between the vertical lines shown in Figure 4, for two  $T_{it}$ : 100 and 129°C.

The parameters  $n$  and  $K$  are depicted in Figure 5 as a function of the  $T_{it}$ . The Avrami exponents

shown in Figure 5(A) correspond to the slopes of the plots shown in Figure 3(B) and the kinetic constant [Fig. 5(B)] corresponds to the Y-intercept in Figure 3(B).

The value of the Avrami exponent  $n$  for the  $T_{it}$  at 100°C is almost 40; however, the value of  $n$  decreases as the  $T_{it}$  increases, as shown in Figure 5(A). It may also be observed that  $n$  decreases to a value of 3 as the  $T_{it}$  reaches the isothermal crystallization temperature,  $T_c^*$ .

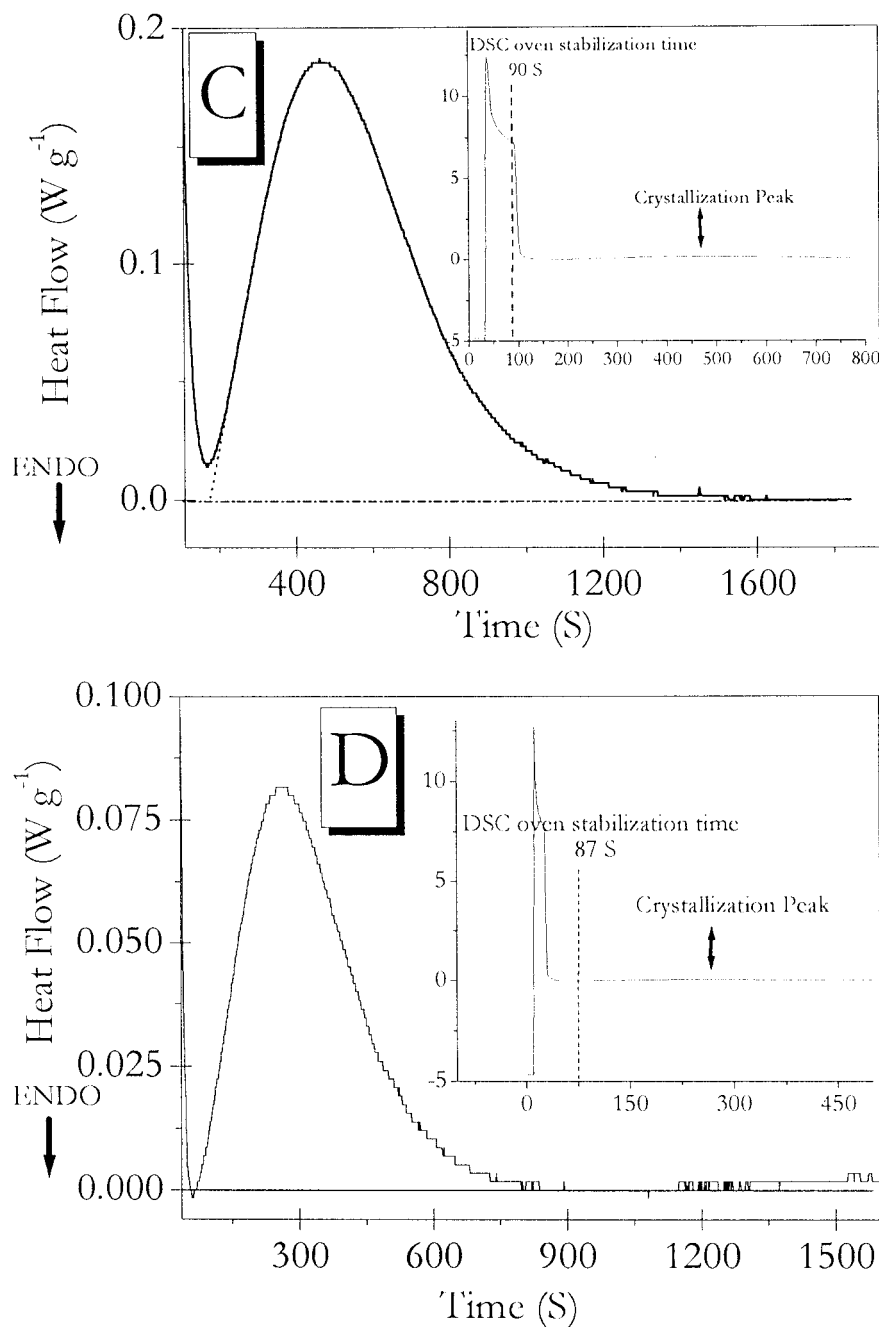


Figure 1 (Continued from the previous page)

A value of  $n = 3$  corresponds to bulk crystallization of pure polymers under isothermal conditions. Under nonisothermal conditions other factors not included in the Avrami model are involved and, consequently, the resulting values of  $n$  may present strong deviations.

Similar arguments should apply for the kinetic constant  $K$ . The values of  $\log(K)$  as a function of  $T_{it}$  are shown in Figure 5(B). As expected, the value of  $K$  increases with  $T_{it}$ . However,  $K$  achieves a constant value as the  $T_{it}$  reaches the  $T_c^*$  of the material.

These results strongly suggest that reliable isothermal experiments can be conducted by DSC only at temper-

atures near the  $T_c^*$ . Only under these conditions does the use of the Avrami model lead to confident results.

In the temperature range where  $n$  and  $K$  change with  $T_{it}$  (Fig. 5), the crystallization experiment is nonisothermal and the kinetic constant could be expressed in the following form:

$$K = K_0 \exp\left[\frac{-E}{R(T_c^* - T)}\right] + K_1 \quad (2)$$

where  $E$  is the activation energy,  $T_c^*$  corresponds to the DSC isothermal crystallization temperature,  $R$  is the

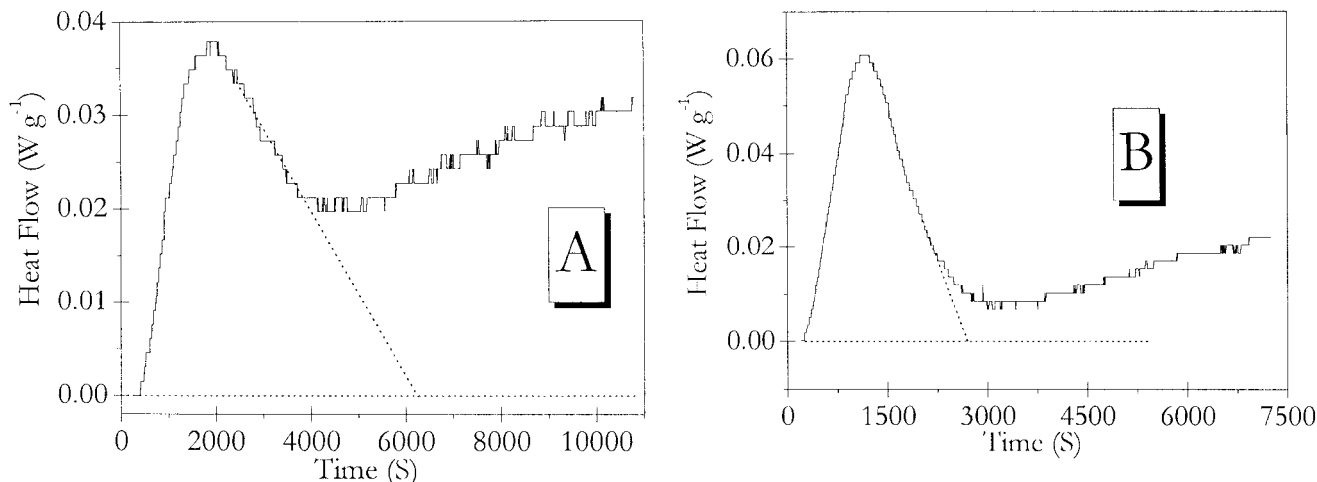


Figure 2 Thermograms for *iPP* at a  $T_{it}$  of 130°C: (A) MW = 50,400, (B) MW = 151,900.

universal gas constant,  $K_1$  is the value of  $K$  at the  $T_c^*$  and  $K_0$  is a fitting-reference parameter. The values of these parameters considering temperatures close to the  $T_c^*$  are  $\log K_0 = -20.6$ ,  $\log K_1 = -9.4$ , and  $E = 2.5R$ .

As may be observed the crystallization kinetics depend on the difference  $T_c^* - T$ . As the  $T_{it}$  increases, the value of  $K$  increases, as shown in Figure 5(B). Therefore the crystallization kinetics can be defined in a form similar to the Avrami model, in terms of nucleation and crystal growth, even for nonisothermal processes.

The kinetics of polymer crystallization is slow compared with that of other types of materials, favoring the experiments by DSC. However, it becomes mandatory to pinpoint the limits for conducting reliable kinetic studies under isothermal conditions by DSC

and by using the Avrami model, as shown here for the case of *iPP*.

The implications of the procedure used for the isothermal experiment by DSC also need discussion. The difference in heat capacities between the sample and the DSC oven leads to a temperature difference between them during the cooling step, particularly at a fast cooling rate. Once the oven reaches the  $T_{it}$  the polymer sample may still be at a higher temperature and cooling at a rate that possibly follows an asymptotic pattern. Therefore, before thermal stabilization occurs at  $T_{it}$ , the signal registered by the DSC is a combination of the thermal stabilization of the oven and the sample. Furthermore, depending on the  $T_{it}$ , the crystallization process may start well before thermal stabilization occurs. This is the case at  $T_{it}$  between

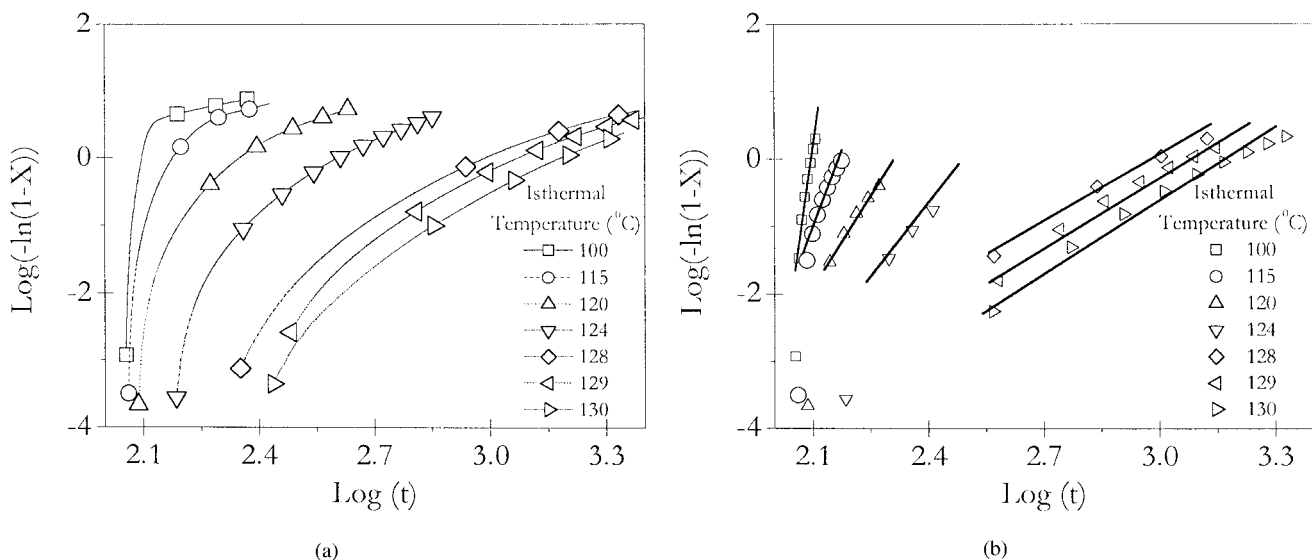
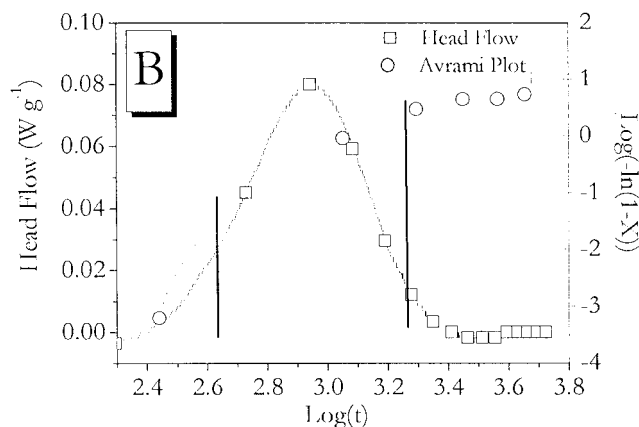
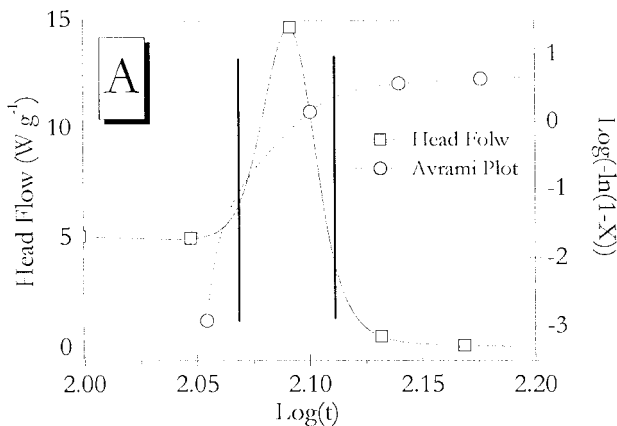
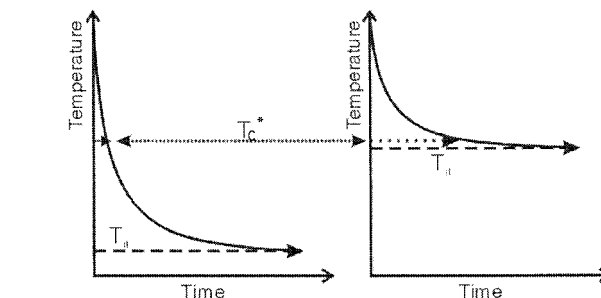
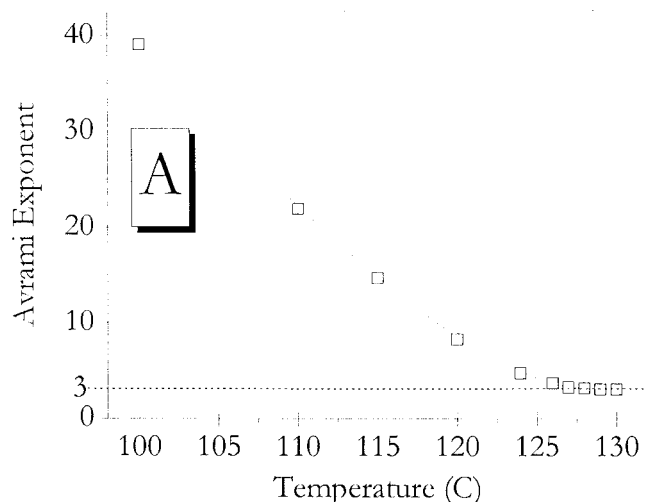


Figure 3 Avrami plot for different  $T_{it}$ : (A) complete data plot, (B) linear sections of the data selected to obtain the Avrami exponent and the kinetic constant.



**Figure 4** Crystallization peaks at two  $T_{it}$ : (A) 100°C and (B) 129°C. The dashed line corresponds to the Avrami plot. The vertical lines correspond to the linear time interval, as shown in Figure 3(B).



**Figure 5** Behavior of the Avrami parameters as a function of  $T_{it}$  for *i*PP of MW 151,900: (A) exponent  $n$  and (B) kinetic constant  $K$ . The dashed line indicates the corresponding representative parameters under isothermal conditions.

**Figure 6** Scheme of the DSC oven cooling at: (A)  $T_{it}$  well below the onset of crystallization and (B)  $T_{it}$  at the onset of crystallization. The dotted line represents the  $T_c^*$  and the dashed line represents the  $T_{it}$ .

100 and 126°C, as depicted in Figure 1(A)–(C). Only at  $T_{it}$  between 127 and 129°C does the crystallization process start at the onset of thermal stabilization [Fig. 1(D)].

These kinetic effects can be explained by the scheme shown in Figure 6. For an experiment at a  $T_{it}$  well below the  $T_c^*$  of the material, the cooling rate of the sample is high (slope of the curve) at the crossing point with the  $T_c^*$  [dashed line in Fig. 6(A)]. Therefore, the delay time between this crossing point and the point at which the temperature of the sample reaches the  $T_{it}$  is also large. Under these conditions the sample starts crystallization well before thermal stabilization and the heat flow is higher than the expected value because of the addition of the heat flow for the thermal stabilization of the oven and the sample, to that of the crystallization process. Therefore, the crystallization peak signal cannot start at zero heat flow and an extrapolation is required to estimate the onset of crystallization and the mass fraction of crystallinity  $X$ .

At a  $T_{it}$  below but near the  $T_c^*$  [Fig. 6(B)], the cooling rate of the sample is small at the crossing point with

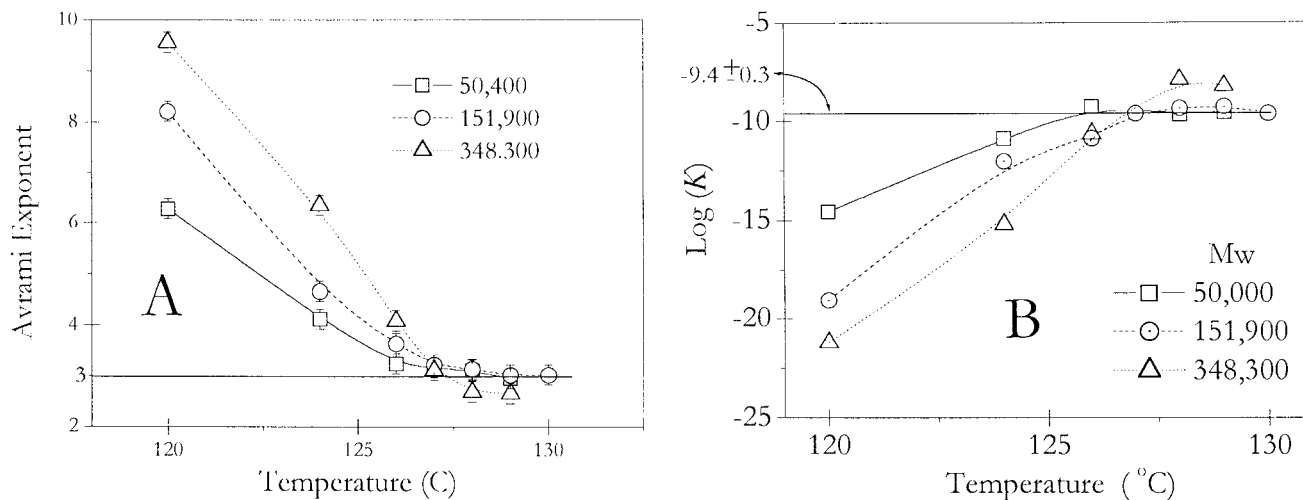


**Figure 7** Avrami parameters of *i*PP of different molecular weights: (□) 50,400, (○) 151,900, and (△) 348,300 as a function of  $T_{it}$ : (A) exponent  $n$  and (B) kinetic constant  $K$ .

the  $T_c^*$  line and the delay time between this crossing point and the point at which the temperature of the sample reaches the  $T_{it}$  is short. Under these conditions, the sample starts crystallization at the onset of thermal stabilization and the crystallization peak signal start at zero heat flow. Therefore, the onset of crystallization and  $X$  can be accurately calculated.

The above discussion leads to the conclusion that, in a strict sense, there is an inherent source of error in isothermal crystallization experiments by DSC. How-

ever, it is possible to approximate the isothermal experiment when the  $T_{it}$  is near the  $T_c^*$  of the material, about 2 or 3°C, depending on the material. In the particular case of *i*PP the range for isothermal experiments is between 127 and 129°C.

#### The effect of molecular weight

The effect of molecular weight on isothermal crystallization kinetics was also studied on *i*PP. Behaviors of

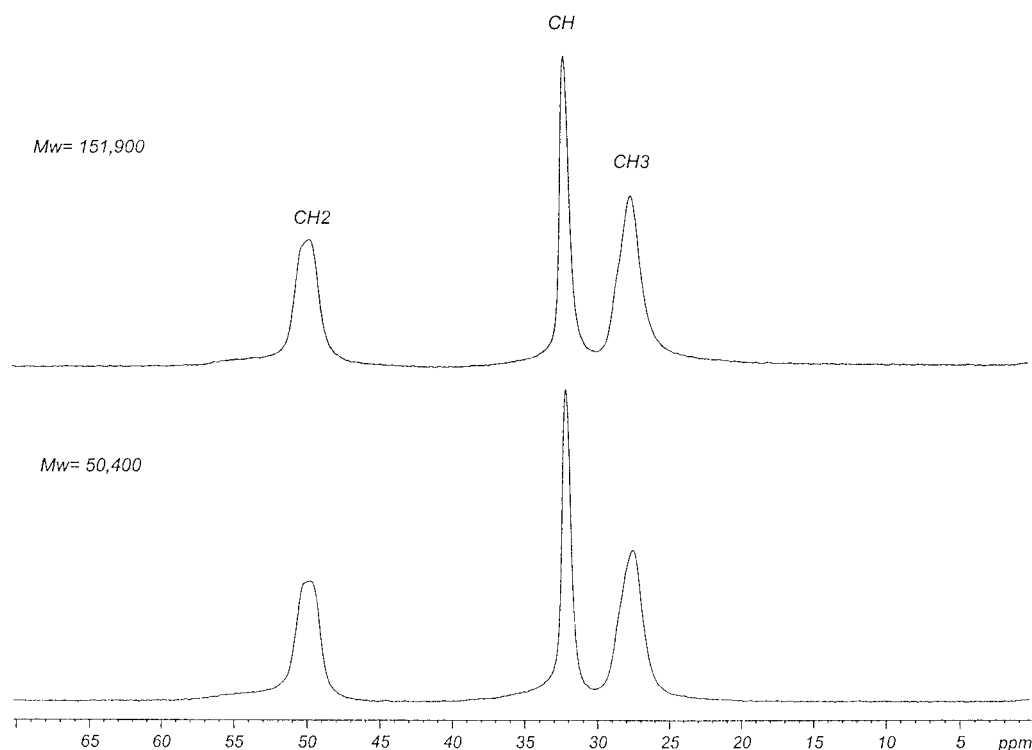


**Figure 8** NMR spectra of polypropylene by solid-state  $^{13}\text{C}$  CP/MAS: (a) MW = 50,400 and (b) MW = 151,900.

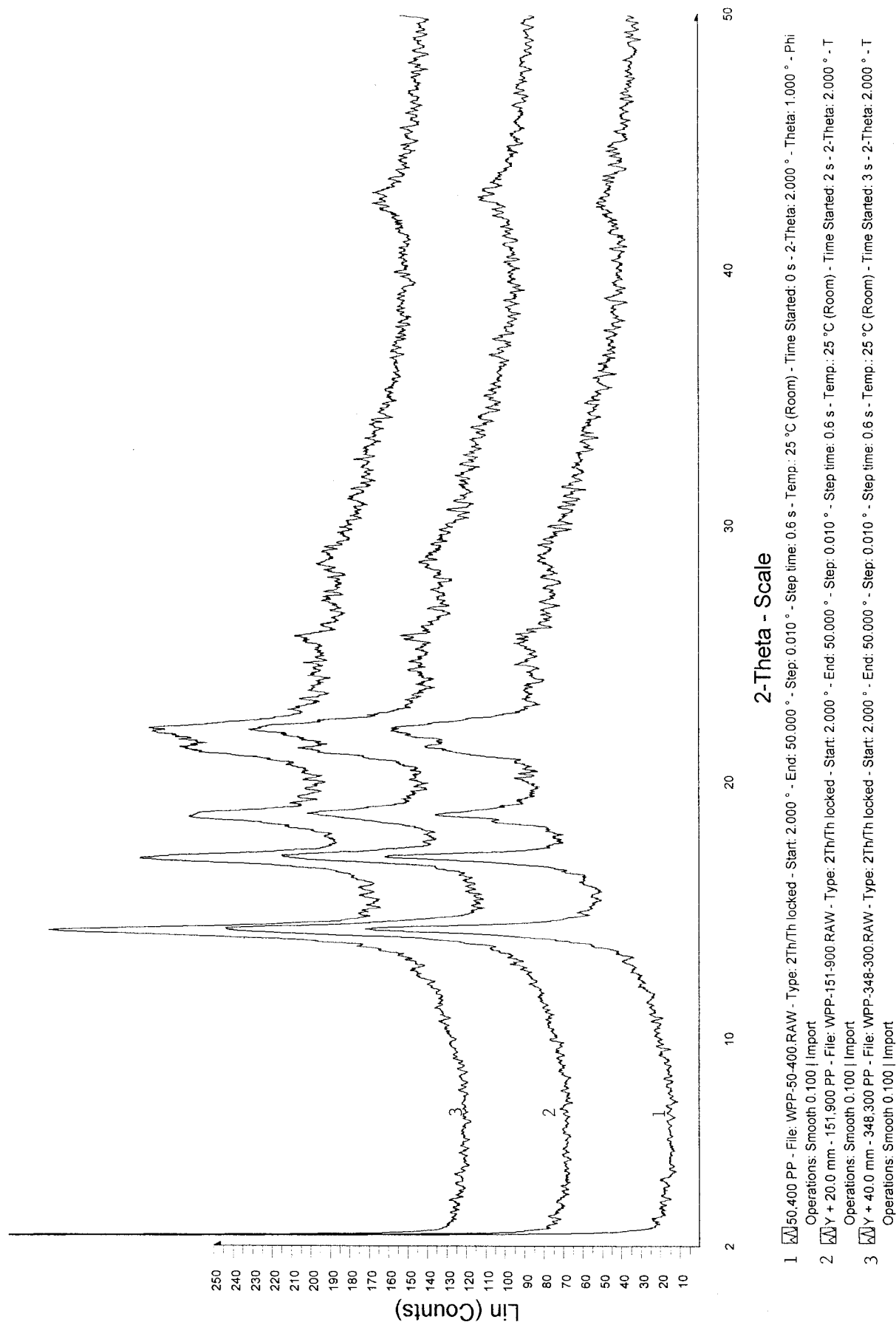


Figure 9 X-ray diffraction spectra of polypropylene: (1) MW = 50,400, (2) MW = 151,900, and (3) MW = 348,300.



the Avrami exponent  $n$  and kinetic constant  $K$  as a function of  $T_{it}$  are shown in Figure 7(A) and (B), respectively, for three MW: 50,400, 151,900, and 348,300. As expected, it can be observed that  $n$  decreases to a value of 3 and  $K$  achieves a constant value as the  $T_{it}$  reaches the  $T_c^*$ , about 128 to 130°C. In this range  $n$  approximates 3 and  $\log(K)$  is equal to 9.4. However, for the sample of lower MW (50,400)  $n = 3$  at 128°C, whereas for the samples of higher MW (151,900 and 348,300)  $n = 3$  at 129°C. These data suggest that the low molecular weight fractions of the polymer may affect the  $T_c^*$ .

Again, at the temperatures where  $n$  and  $K$  change with  $T_{it}$ , the crystallization experiment is nonisothermal and the kinetic constant could be expressed by eq. (2).

An additional evidence of the effect of low molecular weight fractions on crystallization is the thermogram of *i*PP of MW 50,400 at a  $T_{it}$  of 130°C [Fig. 2(B)]. The initial part and the maximum of the crystallization peak are clearly observed, but only a small part of the descendant line is observed; the curve rises again after passing the maximum. This behavior also suggests that the crystallization temperature of this material is somewhat lower than 129°C compared with the descendant line of the peak in Figure 2(A).

A large extrapolation (dotted line) of the descendant part of the peak in Figure 2(B) was required to calculate the crystalline fraction. In this case  $n = 2.2$ . Probably at 130°C crystallization is not three-directional but crystals grow by a diffusion-controlled process, thus reducing the Avrami exponent.<sup>6</sup>

### Characterization of *i*PP

The NMR spectra of the polypropylene samples are shown in Figure 8. Three resonance peaks are observed in the NMR spectra: The peak at 49.7 ppm is assigned to the CH<sub>2</sub> (C1 carbon), the peak at 32.1 ppm to the CH (C2), and the peak at 27.5 to the CH<sub>3</sub> (C3). The spectra were compared to the CP-MAS spectra of polypropylene reported elsewhere and correspond to the isotactic configuration.<sup>7</sup>

The X-ray diffraction spectra of the polypropylene samples are shown in Figure 9. The spectra clearly correspond to isotactic polypropylene and the diffraction patterns do not show evidences of the  $\beta$ -modification in the samples,<sup>8</sup> neither about fractions with syndiotactic configuration.<sup>9</sup> These results and the melting temperature of the polypropylene confirm the purity of the polymer standards used in the study.

### CONCLUSIONS

DSC techniques are very useful in a wide variety of applications; however, the study of isothermal crystallization process by DSC requires careful consideration of inherent and external conditions to obtain reliable

data. We have discussed these conditions for the study of the crystallization kinetics of isotactic polypropylene by DSC. However, the general conditions discussed here should also apply to the study of other polymers.

To define the conditions at which an isothermal crystallization process of a polymer can be analyzed by DSC, it is required to determine the experimental temperature at which the DSC is able to register the crystallization peak from the beginning to the end of the crystallization process. We define this as the "DSC isothermal crystallization temperature." This  $T_c^*$  is an operational temperature because at any other test isothermal temperature the peak registered by the DSC is incomplete. In fact, according to our results for  $T_{it} < T_c^*$  the initial part of the peak does not start at zero heat flow. In contrast, for  $T_{it} > T_c^*$  the end part of the peak does not fall to zero heat flow and the curve rises at some part of the descendant line.

These experimental conditions are also closely related to time required for stabilization of the DSC after the cooling step of the oven to reach the  $T_{it}$ . If that time is shorter than the time to initiate the crystallization process then the crystallization starts under isothermal conditions. Otherwise, the heat flow is a combination of the heats of crystallization and that evolved during stabilization of the oven and the process becomes nonisothermal.

In a strict sense, the Avrami model in its original form is valid under isothermal conditions. When using a DSC, the exponent  $n \rightarrow 3$  when the  $T_{it}$  is equal to or lower than, but very close to, the  $T_c^*$ . The kinetic constant  $K$  also achieves a constant value under the described conditions.

The purity of the standards minimized the presence of side effects in the isothermal crystallization results obtained in this work.

The authors thank Gerardo Cedillo-Valverde and Leticia Baños-Lopez for their contribution in the characterization of the polypropylene samples by NMR and WAXD, respectively; and also acknowledge economic support from DGAPA-UNAM Project IN107502.

### References

1. Wunderlich, B. *Macromolecular Physics*, Vol. 2; Academic Press: New York, 1976.
2. Sperling, L. H. *Introduction to Physical Polymer Science*; Wiley-Interscience: New York, 1992.
3. Cyrus, V. P.; Kenny, J. M.; Vazquez A. *Polym Eng* 2001, 41, 1521.
4. Li, J.; Shanks, R.; Olley, R.; Greenway, G. *Polymer* 2001, 42, 7685.
5. Khanna, Y.; Taylor, T. *Polym Eng Sci* 1998, 28, 1042.
6. Quinn, F.; Mandelkern, L. *Contribution from the Polymer Structures Section; National Bureau of Standards: Washington, DC, 1958.*
7. Bovey, A. F. *Nuclear Magnetic Resonance Spectroscopy*, 2nd ed.; Academic Press: New York, 1988; pp 368–418.
8. Lu, H.; Qiao, J.; Xu, Y.; Yang, Y. *J Appl Polym Sci* 2002, 85, 333.
9. Supaphol, P.; Lin, J. S. *Polymer* 2001, 42, 9617.